Sensitivity analysis of relationship between error motions and machined shape errors in five-axis machining center - Peripheral milling using square-end mill as test case -

Li, Zongze
Sato, Ryuta
Shirase, Keiichi
Ihara, Yukitoshi
Milutinovic, Dragan S.

(Citation)
Precision Engineering,60:28-41

(Issue Date)
2019-11

(Resource Type)
journal article

(Version)
Accepted Manuscript

(URL)
https://hdl.handle.net/20.500.14094/90006659

Highlights:

- A novel sensitivity analysis method to elucidate the relationship between the trajectory error and the error motions for each feed axis in five-axis machine tools is proposed.

- The results of the sensitivity analysis can explain how the error motions influence the motion trajectory in the case of square-end milling on a five-axis machine tool.

- The proposed method can help the users of five-axis machining tools predict the machining errors on the designed surface for each axis error motion.

Research Paper

Sensitivity Analysis of Relationship Between Error Motions and Machined Shape Errors in Five-axis Machining Center - Peripheral Milling Using Square-End Mill as Test Case -

Zongze Li [1)], Ryuta Sato [1)*], Keiichi Shirase [1)]
Yukitoshi Ihara [2)], and Dragan S. Milutinovic [3)]

1) Department of Mechanical Engineering, Kobe University
1-1 Rokko-dai, Nada, Kobe 657-8501, JAPAN
TEL/FAX: +81-78-803-6326
Email: sato@mech.kobe-u.ac.jp

2) Department of Mechanical Engineering, Osaka Institute of Technology
3) Faculty of Engineering, University of Belgrade

Abstract

Five-axis machine tools, consisting of three translational axes and two rotary axes, are increasingly being used for complex surface machining. This paper proposes a new sensitivity analysis method to elucidate the relationship between the tool trajectory error and the error motions of the feed axes. Based on the free-curve trajectory during simultaneous five-axis machining, a surface coordinate system is created for each tool center point, to define the tool trajectory and the trajectory errors. Then, a novel sensitivity coefficient is defined to investigate the relationship between the trajectory error and the error motions. It is shown that the proposed sensitivity analysis method can successfully determine whether the trajectory is sensitive to the error motions, based on sensitivity analyses performed during conic frustum machining and S-shaped machining tests. Moreover, the sensitivity analysis method can also predict the effects of the error motion source, such as the reversal errors. In the future, we intend to study other types of machining processes, such as ball-end milling, as well.

Keywords: five-axis machine tools, square-end milling, sensitivity analysis, error motion, surface coordinate system

1 Introduction

With the rapid developments made in the industry and in technology in general over the last few years, the requirements for the manufacturing field are also becoming increasingly complex. As a result, five-axis machine tools are now being used in all areas of manufacturing. In fact, the research and development of five-axis machine tools and their production have become the core focus of manufacturing in several countries. In most instances, five-axis machine tools can be classified into two types: horizontal and vertical, based on the original location of the spindle [1, 2, 3]. In most cases, both types contain three translational axes and two rotary axes. These axes control not only the linear displacement but also the angular displacement between the tool and the workpiece, leading to greater versatility and flexibility and higher machining efficiency, especially with respect to the machining of workpieces with complex curved surfaces, such as impellers and turbine blades [4, 5, 6]. However, because of the complexity of the machine tool structure, a critical issue with five-axis machine tools is the machining accuracy. Compared to conventional three-axis machine tools, five-axis machine tools have more sources of errors as per the ISO 230-1 standard [7].

To improve the accuracy of five-axis machine tools, it is necessary to evaluate their error sources correctly. For this, two methods can be used: the first one requires the use of professional instruments such as a "double ball-bar" or an "R-test," while the second one involves performing a specific machining test [7, 8, 9]. Professional instruments, such as the ball-bar, are already being used throughout the world but are very expensive for most machine tool users and manufacturers. Moreover, the detection results obtained using a ball-bar system are sometimes not easy to interpret. In addition, the geometric errors detected using the no-load method may be significantly different from those corresponding to normal operational conditions [10]. Therefore, a machining test is better suited for evaluating the machining accuracy of five-axis machine tools. Thus, a variety of machining tests have been developed based on the ISO 10791-7 standard. The most widely used one is the M3 test, which involves the use of a conic frustum and was first presented as the NAS 979 test [9, 11]. It has been shown that the conic frustum cutting test is suitable for evaluating the performance of five-axis machine tools and that this test can be performed using a double ball-bar system [12, 13]. In addition, the S-shaped machining test, proposed by AVIC Cheng Du Aircraft Industrial Co. Ltd., is a modified version of the test proposed in the ISO 10791-7 standard [9]. The S-shaped machining test holds a thin wall, variable curvature, variable tilt angle and other characteristics which satisfied suitably by aero manufactures. Jiang et al. [14] reported that S-shaped machining can be used to evaluate the dynamic performance of the servo system of five-axis machining centers based on a comparison of the results of simulations of S-shaped machining and the NAS 979 test.

However, in case of these tests, the error sources in five-axis machine tools may cause deviations in the tool trajectory. Thus, it is important for machine tool manufacturers and researcher to elucidate how individual errors affect the tool trajectory.

It is also expected that the effects of the various error sources on the accuracy of the machined shape will not be the same, given the relationship between the direction of the error sources and the geometry of the machined specimen [15, 16]. For this purpose, the most suitable method would be to perform a sensitivity analysis for each error source. Sensitivity analyses allow one to investigate the effects of parameter changes on mathematical models [17] and have been used in a range of fields, including economics, biology, chemistry, and engineering. In most instances, sensitivity analyses can be classified either as local sensitivity analyses or global sensitivity analyses [18, 19, 20]. A local sensitivity analysis evaluates the deformation caused by tiny changes in individual parameters, while a global sensitivity analysis can explain how the model response changes with the system variables. As the response is usually dependent on several factors, sensitivity analysis is an effective method for dividing the synthetic response into individual components, to determine the individual contribution of each affecting factor. In the field of machine engineering, sensitivity analyses have been widely used for analyzing machining errors and on-machine measurements. Chen et al. [5] performed a sensitivity analysis of the volumetric error for 37 error components and could improve the design and manufacturing accuracy of a five-axis ultraprecision machine tool. Kato et al. [13] used the ratio of the measurement value to the actual error as the sensitivity coefficient and used this coefficient to interpolate the three-dimensional circular movement of a machining system. Cheng et al. [20] reported a new analysis method based on the multibody system theory and performed a global sensitivity analysis to identify the most important geometric errors affecting the machining accuracy of multi-axis machine tools. Ibaraki et al. [21] used a kinematic model to perform an error sensitivity analysis of on-machine measurements and evaluated the contributions of the position and orientation errors as well as the geometric errors of the rotary axes to the measured profiles, in order to determine whether it is possible to track the on-machine measurements with the rotation of the workpiece. Cheng et al. [22] developed a model for determining the machining accuracy reliability and performed a sensitivity analysis of machine tools based on the multibody system theory as well as a Monte Carlo simulation to determine the accuracy of quality control of machined products. However, no study has elucidated the relationships between the error sources and the geometry of the machined specimen while taking into account the tool path and geometry.

This paper proposes a novel method for performing a sensitivity analysis of the relationship between the error motions and the error in the machined shape in case of peripheral milling with a square-end mill using a five-axis machine tool. The sensitivity analysis method is based on the Denavit-Hartenberg (D-H) matrix and the kinematics of the machining motions. The error motion of each axis is considered individually, and a new sensitivity coefficient is defined to evaluate the effect of these motions. Two different machine tests—the conic frustum machining test and the S-shaped machining test— are used to produce the test samples. Furthermore, the effect of the reversal motion errors of the axes is used to confirm the suitability of the defined sensitivity coefficient.

The rest of the manuscript is organized as follows. The error motions of five-axis

machine tools are described based on the relevant ISO standards in Chapter 2. Chapter 3 introduces the machining errors and the sensitivity coefficient used. The results of the sensitivity analyses of the conic frustum machining test and the S-shaped machining test are discussed in Chapters 4 and 5, respectively. The results of simulations of the reversal motion errors performed to verify the results of the sensitivity analyses are also discussed in these chapters. Finally, the conclusions are presented in Chapter 6.

2 Error motions in five-axis machining centers

2.1 Definition of error motions

During machining using a machine tool, there will always occur unwanted linear and angular motions of the linear axes moving along a straight path or the rotary axes moving around an angular path; these unwanted motions are called error motions. These error motions may arise from the geometric errors of the guide ways or bearings or from the dynamic mechanical parts [23]. Normally, there are six directions of freedom for a kinetic component. Thus, for each axis, six error motions must be considered. These six error motions and their characteristics are defined by ISO standards [7]. For the linear axes, such as the X-axis, the error motions are as given in **Figure 1**, while for the rotary axes, such as the C-axis, the error motion are as given in **Figure 2**. Further, descriptions of the various errors are given in **Tables 1** and **2**.

Table 1. Descriptions of error motions of X-axis

Symbol	Description
E_{AX}	Angular error motion around A-axis (roll)
E_{BX}	Angular error motion around B-axis (yaw)
E_{CX}	Angular error motion around C-axis (pitch)
E_{XX}	Linear positioning error motion of X-axis; positioning deviations of X-axis
E_{YX}	Straightness error motion in Y-axis direction
E_{ZX}	Straightness error motion in Z-axis direction

Table 2. Descriptions of error motions of C-axis

Symbol	Explanation
E_{XC}	Radial error motion of C-axis in X-direction
E_{YC}	Radial error motion of C-axis in Y-direction
E_{ZC}	Axial error motion of C
E_{AC}	Tilt error motion of C around X-axis
E_{BC}	Tilt error motion of C around Y-axis
E_{CC}	Angular positioning error of C; measured angular positioning deviations of C-axis

2.2 Transformation of error motions in five-axis machining center

In this study, we focused on the linear positioning error motion of the linear axes and the angular positioning error motion of the rotary axes. Although other error motions also exist, as mentioned above, we chose the individual error motions of each axis to evaluate the effectiveness of the proposed sensitivity coefficient, which is described below. Sensitivity analyses of the other error factors will be performed in a later study.

In the case of a five-axis machine tool with a tilting rotary table with a B-axis and a C-axis, as shown in **Figure 3** (a), five types of motion errors, namely, E_{XX}, E_{YY}, E_{ZZ}, E_{BB}, and E_{CC}, must be considered, as shown in **Figure 3** (b). Based on the D-H matrix, the transformation of the error motions from the machine coordinate system to the table coordinate system can be done using Equation (1):

$$\begin{bmatrix} x_t \\ y_t \\ z_t \\ 1 \end{bmatrix} = \begin{bmatrix} \cos(C + E_{CC}) & -\sin(C + E_{CC}) & 0 & 0 \\ \sin(C + E_{CC}) & \cos(C + E_{CC}) & 0 & 0 \\ 0 & 0 & 1 & 0 \\ 0 & 0 & 0 & 1 \end{bmatrix} \cdot \begin{bmatrix} \cos(B + E_{BB}) & 0 & 0\sin(B + E_{BB}) & 0 \\ 0 & 1 & 0 & 0 \\ -\sin(B + E_{BB}) & 0 & \cos(B + E_{BB}) & 0 \\ 0 & 0 & 0 & 1 \end{bmatrix} \cdot \begin{bmatrix} x_m + E_{XX} \\ y_m + E_{YY} \\ z_m + E_{ZZ} \\ 1 \end{bmatrix} \quad (1)$$

where $\begin{bmatrix} x_m \\ y_m \\ z_m \end{bmatrix}$ is the tool tip under the machine coordinate system and $\begin{bmatrix} x_t \\ y_t \\ z_t \end{bmatrix}$ is that under the table coordinate system, while B and C are the rotary angles of the B-axis and C-axis, respectively. Further, the error motion can be transformed from the table coordinate system to the workpiece coordinate system using Equation (2):

$$\begin{bmatrix} x_w \\ y_w \\ z_w \\ 1 \end{bmatrix} = {}^{W}_{T}X \cdot \begin{bmatrix} x_t \\ y_t \\ z_t \\ 1 \end{bmatrix} \quad (2)$$

where ${}^{W}_{T}X$ is the coordinate transformation matrix for the transformation from the table coordinate system to the workpiece coordinate system, and $\begin{bmatrix} x_w \\ y_w \\ z_w \end{bmatrix}$ is the tool tip under the workpiece coordinate system with the motion errors. When $E_{XX} = E_{YY} = E_{ZZ} = 0$ and $E_{BB} = E_{CC} = 0$, $\begin{bmatrix} x_w \\ y_w \\ z_w \end{bmatrix}$ is the tool tip position without any errors. Then, the error motions of each axis can be transformed into the tool path with errors.

3. Definition of sensitivity coefficient

3.1 Definition of surface coordinate system

In most cases, the tool motion trajectories of five-axis machine tools are free-curve trajectories, whose tangential and normal directions are inconstant. Hence, using the table coordinate system or the workpiece coordinate system to define the direction of the machined surface may result in confusion. In this study, we adopted the Frenet frame to define the surface coordinate system, as this has been shown to be an efficient method for describing the free-curve paths of tools [24, 25, 26].

The Frenet frame can describe a free curve using three parameters: the tangential direction, normal direction, and binormal direction. In case of square-end milling, the three directions can be described directly. The tangential direction can be expressed as the vector from a center point of the tool to the next one, so that the tangential unit vector can be defined as given in Equation (3):

$$\overrightarrow{t(n)} = \frac{P_0(n+1) - P_0(n)}{|P_0(n+1) - P_0(n)|} \tag{3}$$

where $P_0(n)$ is the nth center point of the tool under the workpiece coordinate system. In the case of square-end milling, it can be assumed that the spindle is perpendicular to the feed direction. Then, the binormal unit vector can be defined as given in Equation (4):

$$\overrightarrow{b(n)} = [i_n, j_n, k_n] \tag{4}$$

where $[i_n, j_n, k_n]$ are the tool posture data transformed from the table coordinate system to the workpiece coordinate system. The normal unit vector is defined by the tangential unit vector and the binormal unit vector. However, in the case of square-end milling, the normal unit vector will depend on the machining side: for up-cutting, the normal unit vector can be defined as given in Equation (5):

$$\overrightarrow{n(n)} = \overrightarrow{t(n)} \times \overrightarrow{b(n)} \tag{5}$$

In contrast, for down-cutting, the normal unit vector could be defined as given in Equation (6):

$$\overrightarrow{n(n)} = -\overrightarrow{t(n)} \times \overrightarrow{b(n)} \tag{6}$$

Both up-cutting and down-cutting are illustrated in **Figure 4**, and the surface coordinate system defined based on the three unit vectors of all the tool center points is shown in **Figure 5** (up-cutting is taken as the example). In this study, the surface coordinate system was defined as this Frenet frame, and the error motions were analyzed under the surface coordinate system.

3.2 Tool position error in surface coordinate system

For the error motion of a five-axis machine tool, the referred tool position and the actual tool position are as shown in **Figure 6** (a), where P_0 is the referred tool position and P is the actual tool position. The tool position error can then be defined as given in

Equation (7)

$$\overrightarrow{E(n)} = P(n) - P_0(n) \tag{7}$$

In this case, the tool position error can be defined in the surface coordinate system as shown in Equations (8) to (10).

$$E_n(n) = \overrightarrow{E(n)} \cdot \overrightarrow{n(n)} \tag{8}$$

$$E_t(n) = \overrightarrow{E(n)} \cdot \overrightarrow{t(n)} \tag{9}$$

$$E_b(n) = \overrightarrow{E(n)} \cdot \overrightarrow{b(n)} \tag{10}$$

For the actual machining process, the three directional errors would be the exterior normal error, the tangential error, and the spindle directional error, as shown in **Figure 6** (b).

According to Equations (8) to (10), all three errors would have positive or negative values. Thus, for the sake of simplicity, we assumed the following:

- If the error has a positive value, it will be called a positive error.
- If the error has a negative value, the error will be called a negative error.

The sign of the error indicates what type of error it is, with the error type determining the effect of the error on the machining surface. For example, a positive normal error would mean that the machining surface will not be machined adequately and that there would be material to be removed remaining on the machining surface. In contrast, a negative normal error would mean that the machining surface was overcut during the machining process, as shown in **Figure 7**.

3.3 Definition of sensitivity coefficient

To analysis how each error motion affects the accuracy of the machined shape, in this study, we simulated each error motion individually. It was assumed that the overall machining error was caused by the individual error motions. Further, each error motion was kept constant, so that the machining error attributable to the individual error motions could be calculated. Therefore, the sensitivity coefficient was taken to be the quotient of the machining error and the effective error motions, as given in Equation (11):

$$k(n) = \frac{\left|\overrightarrow{E(n)}\right|}{E_{**}} \tag{11}$$

where *k(n)* is the sensitivity coefficient of the position error of each tool tip, $\overrightarrow{E(n)}$ is the position error in Equation (7), and E_{**} is the symbol for the error motion (e.g. E_{XX}). In addition, the sensitivity coefficients for the three components of the position error in the surface coordinate system can be defined similarly, as shown in Equations (12) to (14):

$$k_n(n) = \frac{E_n(n)}{E_{**}} \tag{12}$$

$$k_t(n) = \frac{E_t(n)}{E_{**}} \tag{13}$$

$$k_b(n) = \frac{E_b(n)}{E_{**}} \tag{14}$$

where $k_n(n)$ is the normal sensitivity coefficient, $k_t(n)$ is the tangential sensitivity coefficient, and $k_b(n)$ is the spindle directional sensitivity coefficient.

The sensitivity coefficient is indicative of how the error sources affect the machining accuracy. For an individual error motion, the position error will be large when the sensitivity coefficient is large and small when the coefficient is small. As per Equations (12) to (14), the normal sensitivity coefficient, tangential sensitivity coefficient, and spindle directional sensitivity coefficient are either positive or negative. This means that, when the sensitivity coefficient is positive, a positive axial error motion would cause a positive error and a negative axial error motion would cause a negative error. Similarly, when the sensitivity coefficient is negative, a positive axial error motion would cause a negative error and a negative axial error motion would cause a positive error. Therefore, the sensitivity coefficient as defined in this study reflects not only the magnitude of the machining error caused by the axial error caused but also its direction.

3.4 Example of sensitivity analysis for two-axis motions in X-Y plane

In the previous sections, we introduced the three different sensitivity coefficients. However, it remains to be seen whether all three are significant with respect to the sensitivity analyses performed in this study. In this section, we describe how the defined sensitivity coefficient can be used for sensitivity analysis, based on examples involving square and circular motions in the X-Y plane using two translational axes.

3.4.1 Square motion in X-Y plane

Figure 8 shows the square motion with error motions E_{XX}, E_{YY}, and E_{ZZ}, where the value of each error motion is set to be 0.01 mm (constant), and the error is magnified by a factor of 200. Each motion commenced at point (-25.0, 25.0), and the tip moved in the counter-clockwise direction. The sensitivity coefficients for each error motion are shown in **Figure 9**. As can be seen from **Figure 8** (a), error motion E_{XX} caused a positive error in the trajectory from 50 mm to 100 mm, a negative error from 150 mm to 200 mm, and no error in the other areas. This error range was evaluated using the normal sensitivity coefficient shown in **Figure 9** (a). In addition, it can be seen from **Figure 8** (b) that error motion E_{YY} caused a positive error in the trajectory from 100 mm to 150 mm, a negative error from 0 mm to 50 mm, and no error in the other areas. This error range was also

evaluated using the normal sensitivity coefficient shown in **Figure 9** (b). However, error motion E_{ZZ} caused no error in the motion trajectory, as in the case for square-end milling, error motion E_{ZZ} is always along the spindle direction and thus no error would be transmitted onto the machined surface. This fact can be confirmed from the sensitivity coefficients shown in **Figure 9** (c).

In actual machining operations, the error motions should be position-dependent functions; they can be caused at every step involving the dynamics of machine tools. In this study, setting the error motion to be a constant value does not mean that an error analysis for actual machining operations is conducted. We intend to evaluate the type of influence the error motion causes for each tool point. The relationships between the error motion values and the error at each tool point does not change regardless of how the error motion is set; that is, the results show the deviations in each tool point regarding the defined error motions. Furthermore, a sensitivity analysis can be conducted using the relationships between the defined error motions and the deviations in each tool point.

3.4.2 Circular motion in X-Y plane

Similarly, we also performed sensitivity analysis for circular motion in the X-Y plane. The results yielded the same conclusion as in Section 3.3.1.

Figure 10 shows the circular motion with the three error motions. The value in this case was also set to 0.01 mm and kept constant, and the error was magnified by a factor of 200. However, in contrast to the case for the square motion, the direction for the circular motion was the clockwise direction, with the motion commencing at point (25.0, 0.0). The sensitivity coefficient for each error motion is shown in **Figure 11**. It can be seen from **Figure 10** (a) that error motion E_{XX} caused a positive error at the starting position and that the error kept decreasing and ultimately became zero at the end of the first quarter of the motion. Then, the error became positive and kept increasing until the end of the second quarter of the motion. Next, the error started decreasing again and became zero at the end of the third quarter. Finally, the error became positive again and kept increasing till the end of the fourth quarter. This range can also be evaluated using the normal sensitivity coefficient shown in **Figure 11** (a). In addition, the error range of the circular motion with E_{YY}, shown in **Figure 10** (b), also matches the normal sensitivity coefficient shown in **Figure 11** (b).

Based on the results of the analyses of the square and circular motions, it can be concluded that, in case of square-end milling, error motion E_{ZZ} has no effect on the tool trajectory and that only the normal sensitivity coefficient is significant with respect to this analysis. It should also be noted based on **Figure 6** (b) that only the normal error of the tool path is transferred to the machined surface by the motions during square-end milling. In the next section, therefore, we only analyzed the normal sensitivity coefficient during the sensitivity analysis and ignored error motion E_{ZZ}.

4. Sensitivity analysis of effects of error motions on cone frustum

machining

4.1 Motion during cone frustum machining

According to ISO 10791-7 [9], a cone frustum test can be used with five-axis machining centers to evaluate the cutting performance of the centers under the simultaneous feed motion of the five axes. The structure of the cone frustum test piece is shown in **Figure 12**, while the related parameters are listed in **Table 3**. Both types of cone frustum test pieces described in the table were considered in this study.

In this study, we focused on the M3_15 test to explain the sensitivity analysis. To investigate the influence of the center and the height offset on the sensitivity, conditions both with and without offsets were simulated. The five-axis machine tool used in this study was NMV 1500 DCG, a vertical-type machine tool produced by DMG MORI. The structure of this machine tool is shown in **Figure 3** (a); the tool is holding a rotary tilting table with B- and C-axis. The motion of the feed axes for conic frustum machining is shown in **Figure 13**; the direction of machining is up-cutting. The sensitivity coefficient for each error motion of the axes was analyzed next.

Table 3. Parameters of cone frustum test pieces

Cone frustum parameter	Test piece ISO 10791-7-M3_15	Test piece ISO 10791-7-M3_45
Bottom diameter (D)	80 mm	80 mm
Thickness (t)	20 mm	15 mm
Inclination angle (β)	10°	30°
Half apex angle (θ)	15°	45°
Center offset (d)	25% of diameter of rotary table size (in this study: 62.5 mm)	25% of diameter of rotary table size (in this study: 62.5 mm)
Height offset (p)	Larger than 10% of table diameter (in this study: 30 mm)	Larger than 10% of table diameter (in this study: 30 mm)

4.2 Sensitivity analysis of each error motion

As stated in Section 3, error motion E_{ZZ} can be ignored. Hence, here the sensitivity analysis of X-axis and Y-axis is explained.

Figure 14 and **Figure 15** show the sensitivity coefficients of each error motion of the axes for both without and with offsets. To provide clear results, we have marked the sensitivity coefficients on the motion trajectory, along with the tool tip. If the sensitivity coefficient value is positive, it is marked along the exterior normal direction (the direction of the normal unit vector in Figure 5).

It can be seen that, for the machining test without offset, the sensitivity coefficients

of E_{XX} are always negative, while the sensitivity coefficients for E_{YY} are positive at the region where the Y-coordinate is positive and negative at the region where the Y-coordinate is negative (see **Figure 14**). In addition, the sensitivity coefficients for the rotary axes error motions are approximately equal to 0. In addition, with an offset, according to **Figure 15**, the sensitivity coefficients for the translational axes are the same, while for E_{BB}, the sensitivity coefficients are symmetric to the Y-axis and always negative, with the absolute value increasing along the negative direction of the Y-axis. In contrast, the sensitivity coefficients of E_{CC} are positive in the region where the X-coordinate is negative and positive in the other half. These results show that, for both types of machining, although the motions of the X-axis and Y-axis are different, the sensitivity coefficients are the same. In contrast, for the rotary axes, although the motions are the same, the sensitivity coefficients are different.

4.3 Use of sensitivity analysis to explain influence of reversal errors

As can be seen from **Figure 13**, during both tests, several reversal points existed in the motions, and these reversal points led to reversal errors in the feed drive systems. When the feed motion direction was changed, the error motion occurred during the subsequent motion. Hence, to verify the effectiveness of the sensitivity analysis, the influence of the reversal errors was elucidated based on the sensitivity analysis.

Figure 16 shows the model used to simulate the reversal error; here, a first-order system control mode was used to simulate the servo delay, while a backlash model was used to simulate the reversal errors. The output data from the model were the feed motions, which affected by the backlash.

The trajectories and the effects of the reversal errors are shown in **Figure 17** and **Figure 18**; the trajectory errors are magnified by a factor of 300, and every reversal point is marked on the trajectory. In **Figure 17**, the reversal points on both the X-axis and the Y-axis had some effect on the trajectory in the form of step-like errors, while in **Figure 18**, only the X-axis reversal points had an effect and those on the Y-axis did not. On comparing **Figure 14** and **Figure 15**, it can be seen that all the reversal points during the machining test without an offset were located in the areas where the sensitivity coefficient was large, while for the test with the offset, the Y-axis reversal points were located in the areas where the sensitivity coefficient was not large and thus had no effect.

5. Sensitivity analysis of error motions on S-shaped machining test

5.1 S-shaped machining test

The S-shaped machining test, as shown in **Figure 19 (a)**, is described in the ISO/CD 10791-7 draft standard [9]. The S-shaped test piece consists of two S-shaped ruled surfaces, and the boundary curves of each ruled surface are all three-order uniform rational B-splines. Each B-spline curve is defined by 16 control points. All these parameters are defined in the ISO/CD 10791-7 draft standard [9].

Figure 20 shows the motion feed axes during S-shaped machining using the five-

axis machining center investigated in this study. Because of the stroke limit of the machine tool and the size of the original material, the machining test was carried out using a size that was half of the defined one. The base of the workpiece was also changed suitably; its mechanical drawing is shown in **Figure 19 (b)**. Compared to the motions during conic frustum machining, the motions of the feed axes for S-shaped machining are more complex and approach those involved in the actual machining of complex surfaces. Therefore, the S-shaped machining test can be used to clarify whether the proposed sensitivity analysis method is suitable for analyzing complex surface machining processes as well.

5.2 Sensitivity coefficient of each error motion

As mentioned above, while error motion E_{ZZ} could be ignored, sensitivity analysis was performed for the other four error motions.

Figure 21 shows the sensitivity coefficients for the various error motions of the axes. As was the case in Section 4, the sensitivity coefficients are marked on the motion trajectory, to make the results easy to understand. The numbers shown on the trajectory are indicative of the motion distance from the starting point. As is obvious from the figure, a distinct trend can be seen in the sensitivity coefficients all along the tool trajectory. Thus, the relationship between the trajectory error and the error motion can also be seen clearly. For example, in **Figure 21** (a), the sensitivity coefficient for error motion E_{XX} is positive along the trajectory from 0 mm to 120 mm and decreases from 110 mm. Further, it is almost equal to 0 from 120 mm to 160 mm while beyond 160 mm till the end of the first surface trajectory, it is negative. Hence, it can be concluded that, when E_{XX} = +0.01 mm, a large positive error occurs in the trajectory from 0 mm to 110 mm and a negative error results from 160 mm to the end, with there being no error between 120 mm to 160 mm. Similarly, sensitivity analysis was also performed for E_{YY}, E_{BB}, and E_{CC}.

5.3 Elucidation of effect of reversal errors based on results of sensitivity analysis

As can be seen from **Figure 20**, there were several reversal points in the motions of all the axes. Hence, as was stated in Section 4, the proposed sensitivity coefficient was used to explain the effect of the reversal errors. The method used to simulate the reversal errors was the same as that used in Section 4 (see **Figure 16**).

The trajectories affected by the reversal errors are shown in **Figure 22**; the trajectory errors are magnified by a factor of 200, and every reversal point is marked, as was also done in Section 4.

With respect to the effect of the error motions, as can be seen from **Figure 21** (a), the sensitivity coefficient along the trajectory from 0 mm to 110 mm and from 160 mm to the end of the first surface was large. Thus, the reversal points located in these regions all had pronounced effects (see **Figure 22** (a)). In contrast, from 120 mm to 160 mm, the sensitivity coefficient was almost 0. Thus, the reversal points located in this region did not cause a trajectory error. However, the reversal points still caused error motions. Thus, as soon as the sensitivity coefficient increased, a trajectory error was caused. Further,

there was no reversal point in the region where the X-axis coordinate was approximately 0 on the first surface. Similarly, the reversal errors of the other feed axes can be explained by comparing the corresponding sensitivity coefficient of the error motions.

6. Conclusions

In this study, we proposed a novel sensitivity analysis method to elucidate the relationship between the trajectory error and the error motions for each feed axis in five-axis machine tools. The results of the sensitivity analysis can explain how the error motions influence the motion trajectory in the case of square-end milling on a five-axis machine tool. The primary conclusions of the study can be summarized as follows:

(1) The Frenet frame can be used to define the surface coordinate system, which is more suitable for free-curve tool trajectories. The surface coordinate system is related to each tool center point. Hence, the changed curvature of the tool trajectory has no effect. Further, using the surface coordinate system, the trajectory error could be divided into the normal error, the tangential error, and the spindle directional error.

(2) In case square-end milling, the normal directional error determines the tool trajectory error. It was found that, for every differential of the trajectory, a tangential error occurs along the trajectory, while the spindle directional error occurs along the tool gesture. Further, in the case of square-end milling, these two directions define the differential surface. Moreover, based on an analysis of the square and circular motions, it was determined that only the normal error affects the trajectory errors.

(3) The sensitivity coefficient proposed in this study, which is defined as the quotient of the trajectory error and the effective error motion, can be used to investigate how the error motions affect the tool trajectory. For both the conic frustum machining test and the S-shaped machining test, the sensitivity analysis performed well. In addition, the effects of the reversal errors could also be explained based on the results of the sensitivity analysis.

Thus, it can be concluded that the proposed method can help the users of five-axis machining tools predict the machining errors on the designed surface for each axis error motion. In the future, we plan to explore other types of error motions and machining types, such as ball-end milling, and perform sensitivity analysis, with the aim of developing a global sensitivity analysis method that can be used for all types of machining.

Acknowledgements

The authors would like to acknowledge the support provided by DMG Mori Seiki Co., Ltd. and the Machine Tool Technologies Research Foundation (MTTRF).

References

[1] ISO 10791-1, Test Conditions for Machining Centers- Part 1: Geometric tests for machines with horizontal spindle (horizontal Z-axis), 2014
[2] ISO 10791-2, Test Conditions for Machining Centers- Part 2: Geometric test for machines with vertical spindle or universal heads with vertical primary rotary axis (vertical Z-axis), 2014
[3] Tsutsumi, M., Saito, A., Identification of Angular and Positional Deviations Inherent to 5-axis Machining Centers with a Tilting-rotary Table by Simultaneous Four-axis Control Movements. Int J Mach Tools Manuf; 2004; 1333-1342
[4] Sato, R., Shirase, K., Ihara, Y., Motion Analysis of S-shape Machining Test. Influence of NC Program Quality and Geometric Errors of Rotary Axes on S-shaped Machining Test Accuracy. J Manuf Mat Process 2018; 2; 2; jmmp-272272
[5] Chen, G., Liang, Y., Sun, Y., Volumetric Error Modeling and Sensitivity Analysis for Designing a Five-axis Ultra-precision Machine Tool. Int J Adv Manuf Technol 2013; 68; 2525-2534
[6] Su, Z., Wang, L., Latest Development of a New Standard for the Testing of Five-axis Machine Tools Using an S-shaped Test Piece. Proc IMechE Part B: J Eng Manuf 2015; 1-8
[7] ISO 230-1, Test Code for Machine Tools- Part 1: Geometric Accuracy of Machines Operating under No-load or Quasi-static Conditions, 2012
[8] ISO 10791-6, Test Conditions for Machining Centers- Part 6: Accuracy of Speeds and Interpolations, 2014
[9] ISO/CD 10791-7, Test Conditions for Machining Centers- Part 7: Accuracy of Finished Test Pieces, 2017
[10] Ibaraki, S., Tsujimoto, S., Nagai, Y., Sakai, Y., A Pyramid-shaped Machining Test to Identify Rotary Axis Error Motions on Five-axis Machine Tools: Software Development and a Case Study. Int J Adv Manuf Technol 2018; 94; 227-237
[11] NAS 979: Uniform cutting test- NAS Series, Metal Cutting Equipment Specifications, 1969, 34-37
[12] Kato, N., Tsutsumi, M., Sato, R., Analysis of Circular Trajectory Equivalent to Cone-Frustum Milling in Five-axis Machining Centers Using Motion Simulator. Int J Mach Tools Manuf 2013; 64; 1-11
[13] Kato, N., Tsutsumi, M., Tsuchihashi, Y., Sato, R., Ihara, Y., Sensitivity Analysis in Ball Bar Measurement of Three-Dimensional Circular Movement Equivalent to Cone-Frustum Cutting in Five-axis Machining Centers. J Adv Mech Des Syst Manuf 2013; 7; 317-332
[14] Jiang, Z., Ding, J., Song, Z., Du, L., Wang, W., Modeling and Simulation of Surface Morphology Abnormality of 'S' Test Piece Machined by Five-axis CNC Machine Tool. Int J Adv Manuf Technol 2016; 85; 2745-2759
[15] Sato, R., Nishio, K., Shirase, K., Campatelli, G., Scippa, A., Influence of Motion Error of Translational and Rotary Axes onto Machined Surface Generated by Simultaneous Five-axis Motion. Proc CIRP 2014; 14p; 269-274.
[16] Sato, R., Shirase, K., Geometrical Error Compensation of 5-axis Machining Centers based on On-machine Workpiece Measurement. Int J Auto Technol 2018; 12; 230-237
[17] Turanyi, T., Sensitivity Analysis of Complex Kinetic Systems- Tools and Applications. J

Math Chem 1990; 5;203-248
[18] Sunil, C., Richard, F., Anthony, N., Zhou, Y., Global Sensitivity Analysis for the Determination of Parameter Importance in Bio-Manufacturing Process. Biotechnol Appl Biochem 2008; 51; 79-90
[19] Gianpiero, C., Cosimo, S., Global Sensitivity of a Trophodynamic Model of the Gulf of Trieste. Ecol Model 2008; 212; 16-27
[20] Cheng, Q., Zhao, H., Zhang, G., Gu, P., Cai, L., An Analysis Approach for Crucial Geometric Errors Identification of Multi-Axis Machine Tool Based on Global Sensitivity Analysis. Int Adv Manuf Technol 2014; 75; 107-121
[21] Ibaraki, S., Goto, S., Tsuboi, K., Saito N, Kojima N. Kinematic Modeling And Error Sensitivity Analysis for On-Machine Five-axis Laser Scanning Measurement under Machine Geometric Errors And Workpiece Setup Errors. Int J Adv Manuf Technol 2018; 96; 4051-4062
[22] Cheng, Q., Zhao, H., Zhao, Y., Sun, B., Gu, P., Machining Accuracy Reliability Analysis of Multi-Axis Machine Tool Based on Monte Carlo Simulation. J Intell Manuf 2018 29; 191-209
[23] Kono, D., Matsubara, A., Yamaji, I., Fujita, T., High-precision Machining by Measurement and Compensation of Motion Error. Int. J. Mach Tools Manuf 2008; 48; 1103-1110
[24] Altintas, Y., Khoshdarregi, M.R.，Contour Error Control of CNC Machine Tools with Vibration Avoidance. CIRP Ann-Manuf Technol 2012; 61; 335-338
[25] Altintas, Y., Sencer, B., High Speed Contouring Control Strategy for Five-axis Machine Tools. CIRP Ann-Manuf Technol 2010; 59; 417-420
[26] Yang, J., Altintas, Y., A Generalized On-line Estimation and Control of Five-axis Contouring Errors of CNC Machine Tools. Int J Mach Tools Manuf 2015; 88; 9-23

Figures:

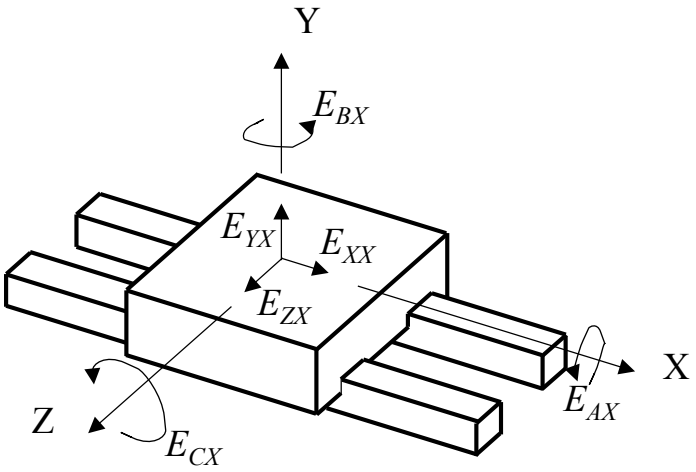

Figure 1 Error motion of X-axis [7].

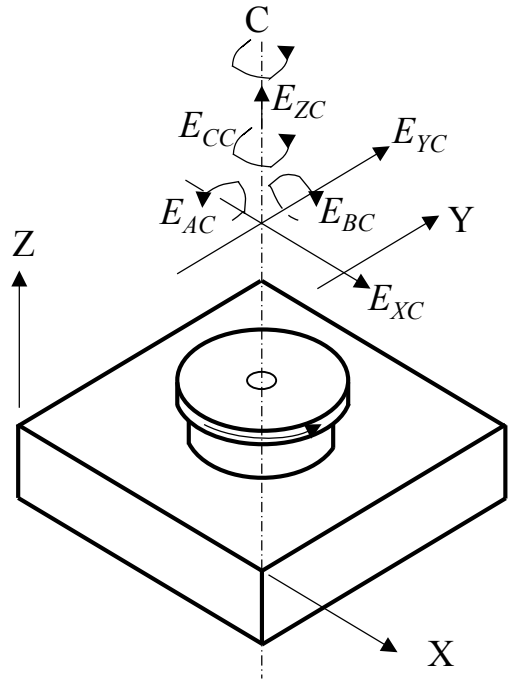

Figure 2 Error motion of C-axis [7].

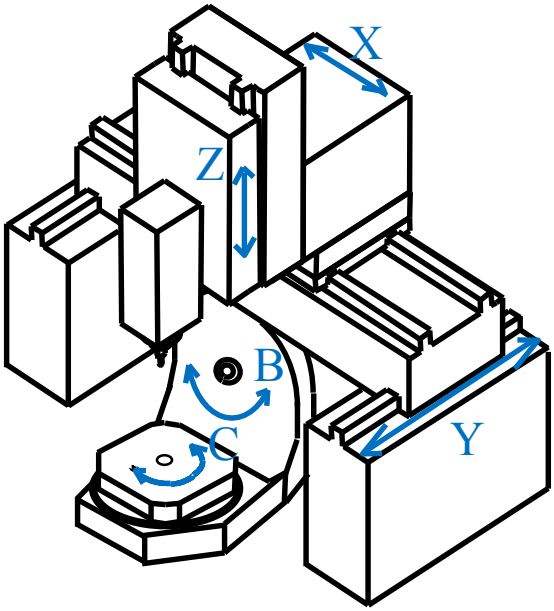

(a) Configuration of five-axis machine tool

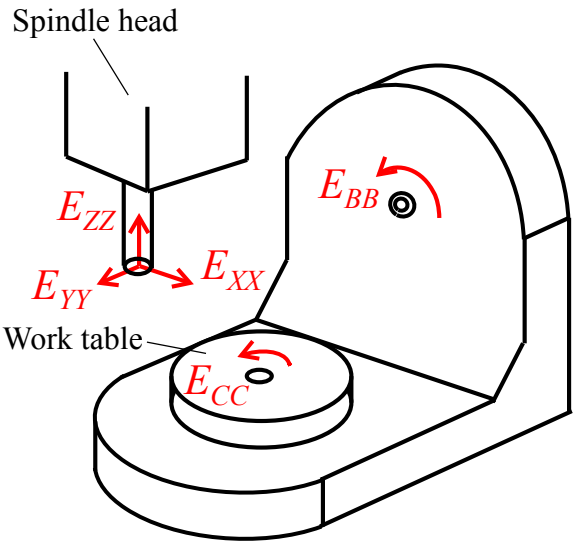

(b) Axial error motions in machine tool

Figure 3 Five-axis machine tool used and error motions analyzed in this study.

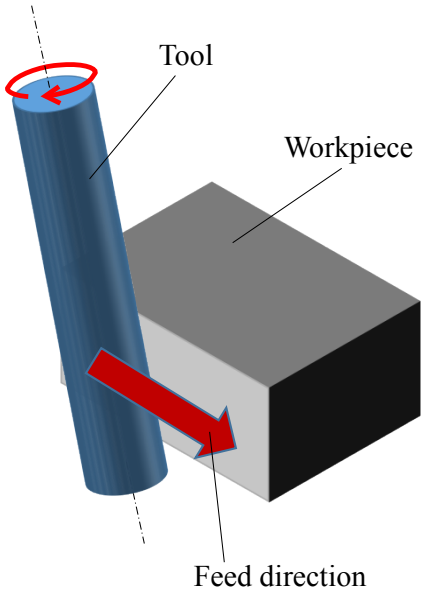

(a) Up-cutting

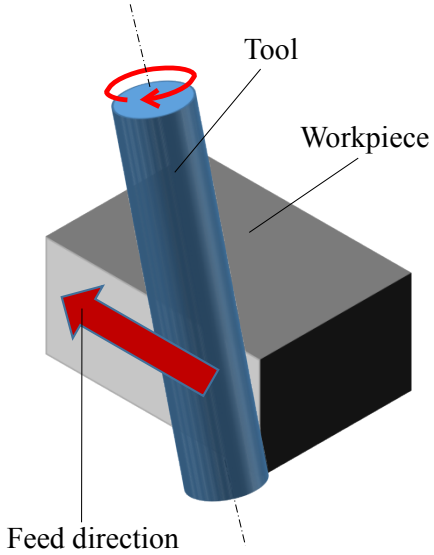

(b) Down-cutting

Figure 4 Up- and down-cutting.

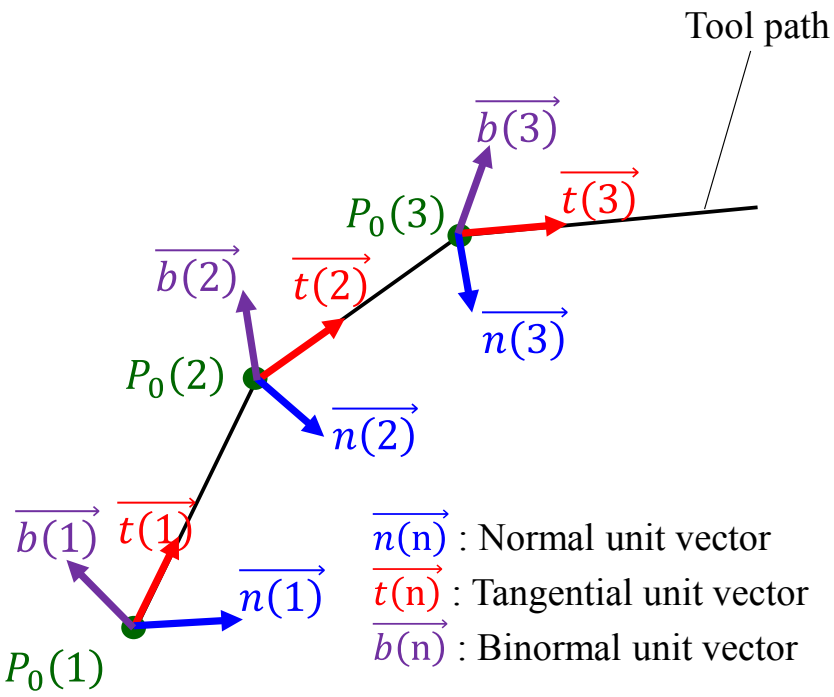

Figure 5 Surface coordinate system.

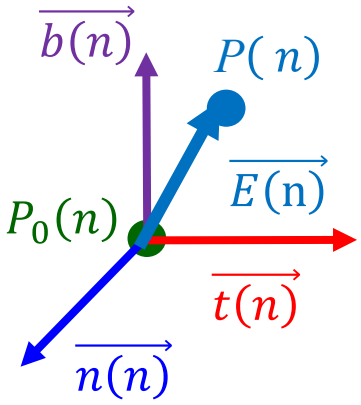

(a) In-surface coordinate system

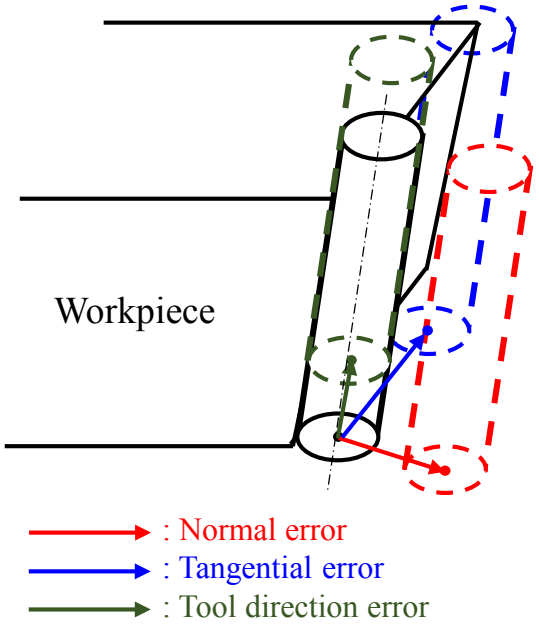

(b) Actual machining process

Figure 6 Tool position error.

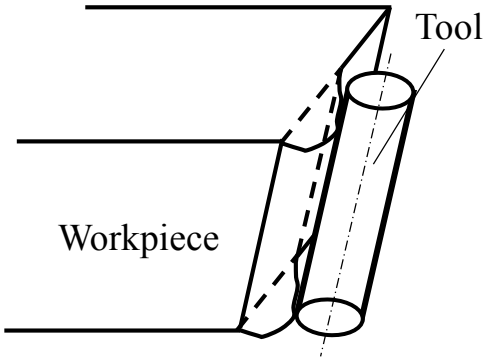

(a) Positive error

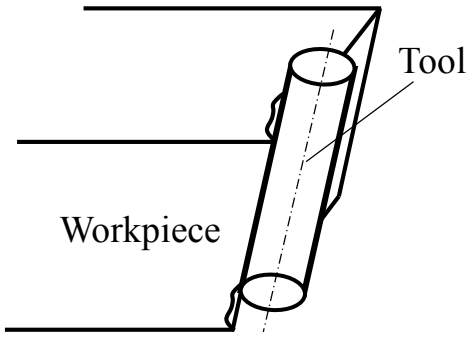

(b) Negative error

Figure 7 Positive and negative errors.

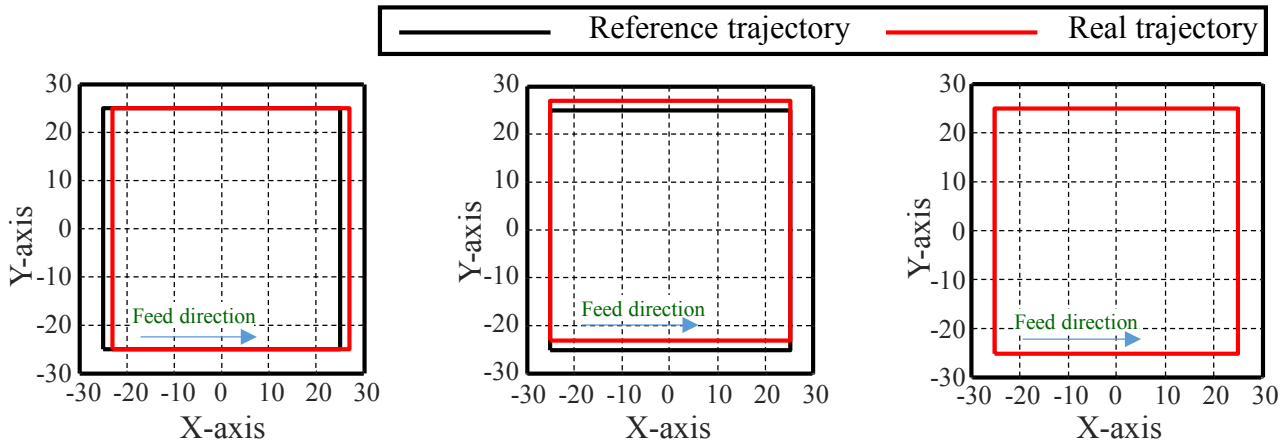

(a) Motion with E_{XX}. (b) Motion with E_{YY}. (c) Motion with E_{ZZ}.

Figure 8 Trajectory errors during square motion.

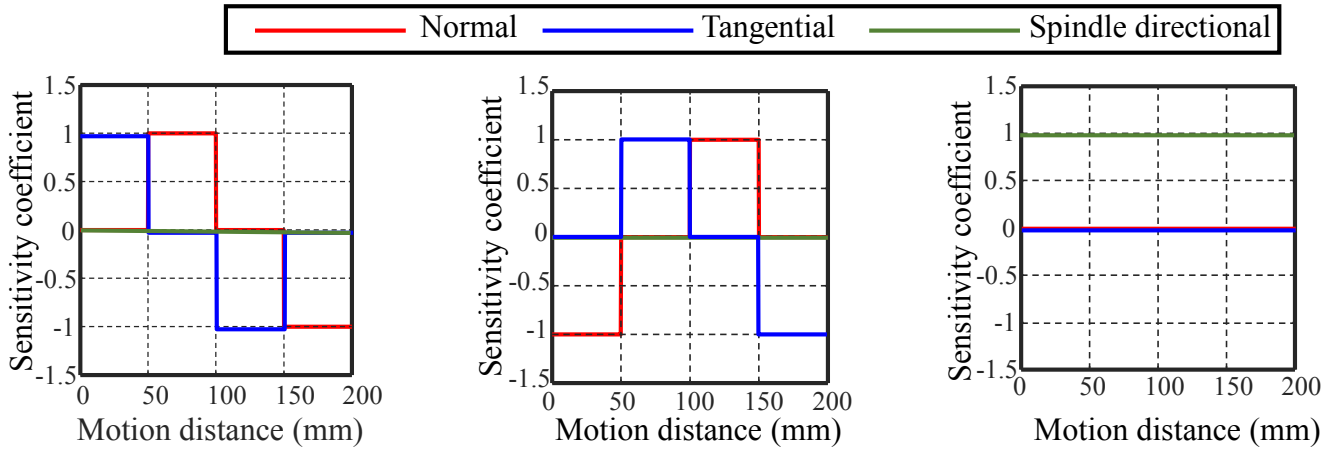

(a) Sensitivity coefficient of E_{XX}. (b) Sensitivity coefficient of E_{YY}. (c) Sensitivity coefficient of E_{ZZ}.

Figure 9 Sensitivity coefficients for square motion.

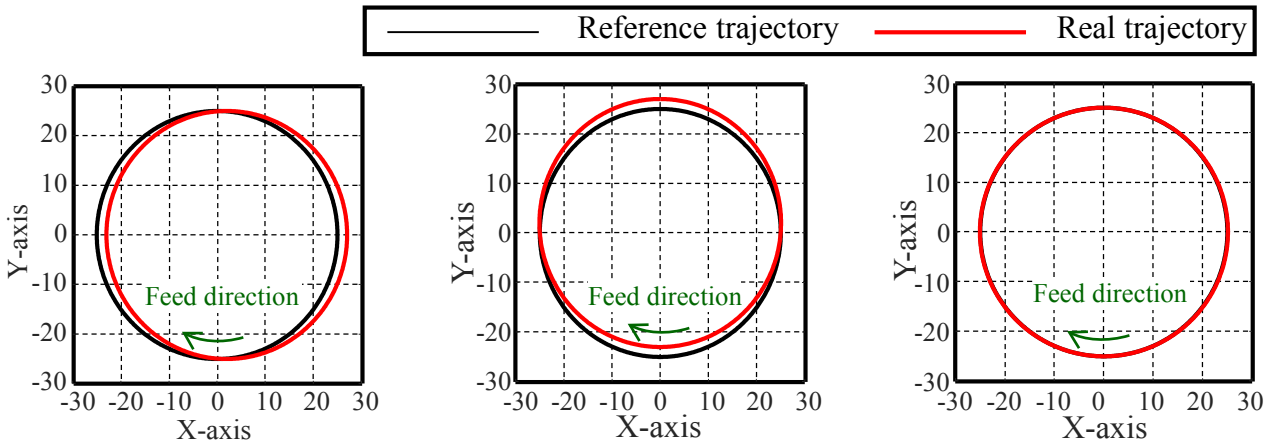

(a) Motion with E_{XX}. (b) Motion with E_{YY}. (c) Motion with E_{ZZ}.

Figure 10 Trajectory errors during circular motion.

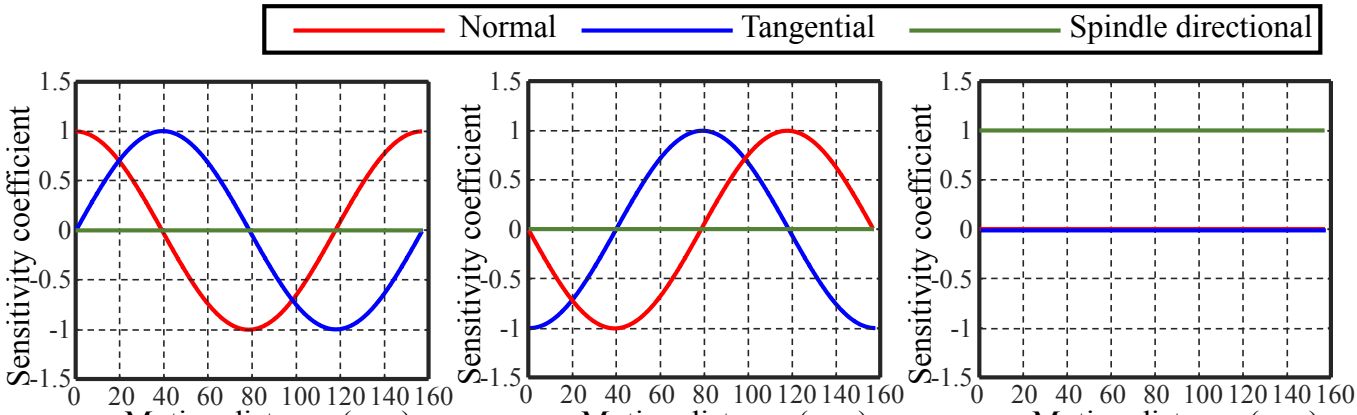

(a) Sensitivity coefficient of E_{XX}. (b) Sensitivity coefficient of E_{YY}. (c) Sensitivity coefficient of E_{ZZ}.

Figure 11 Sensitivity coefficients for circular motion.

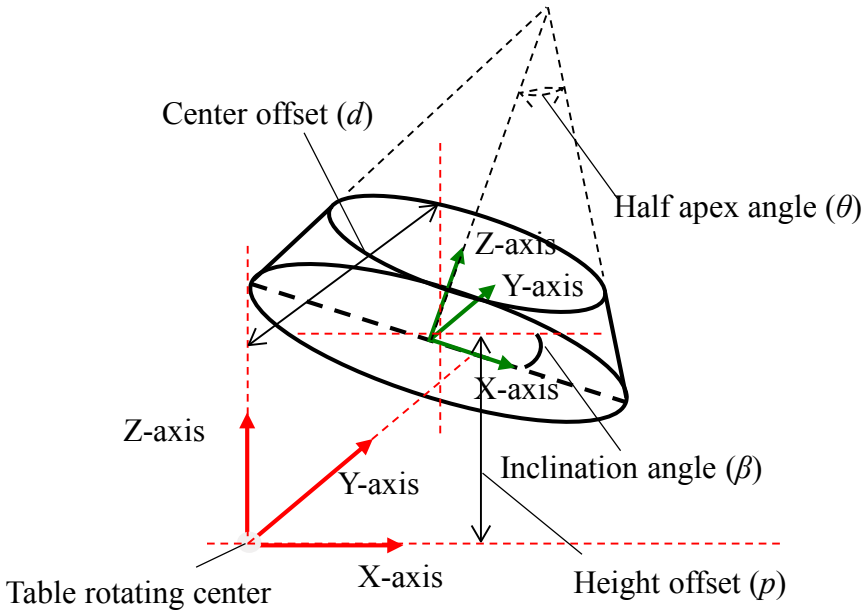

Figure 12 Cone frustum test piece.

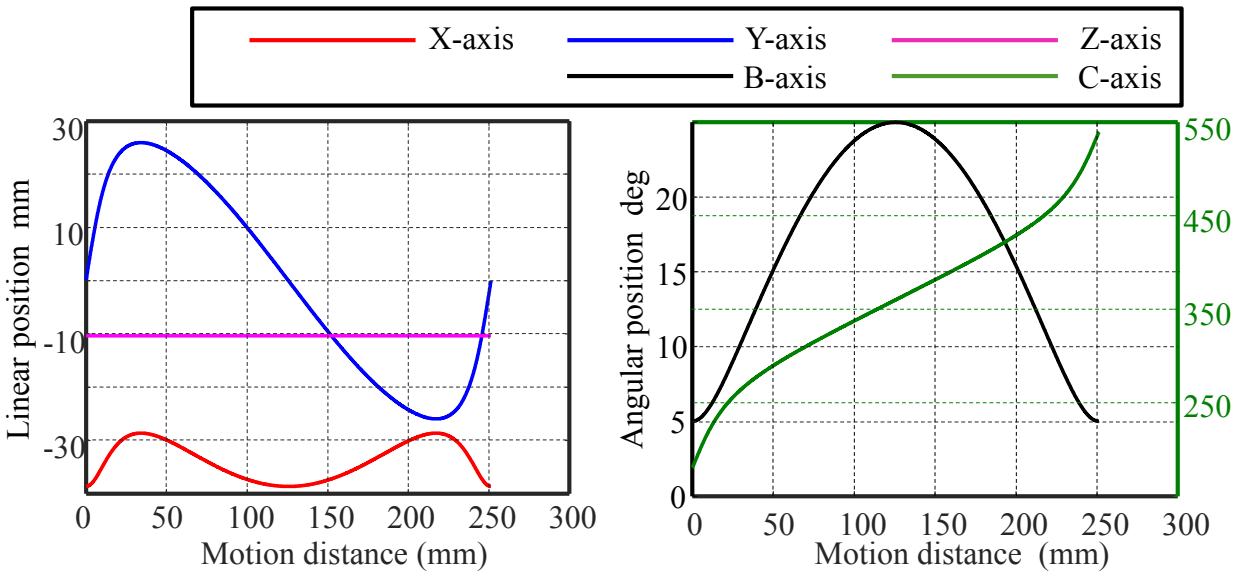

(a) Feed-axes motions of M3_15 test piece without offset.

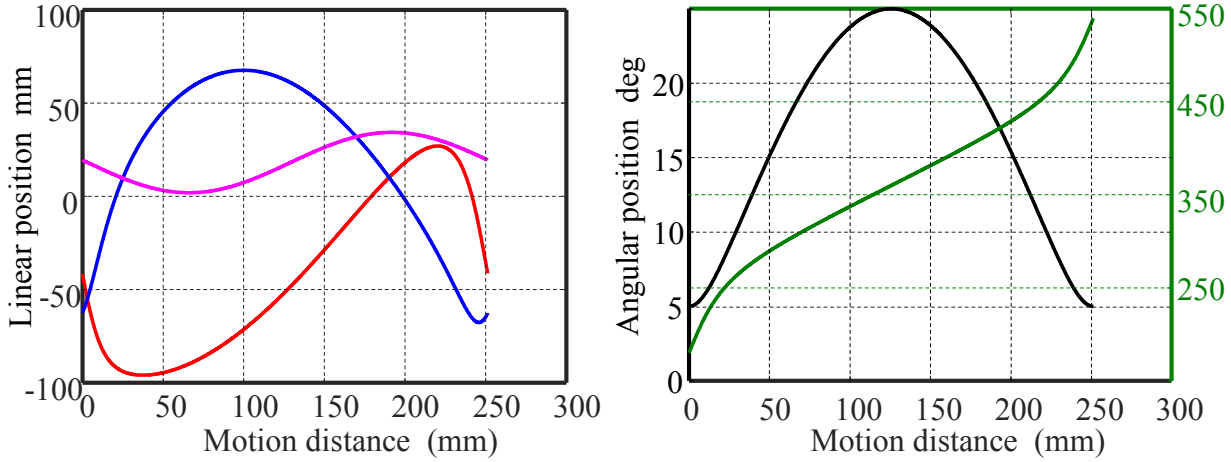

(b) Feed-axes motions of M3_15 test piece with offset.

Figure 13 Feed-axes motions for each conic frustum machining test.

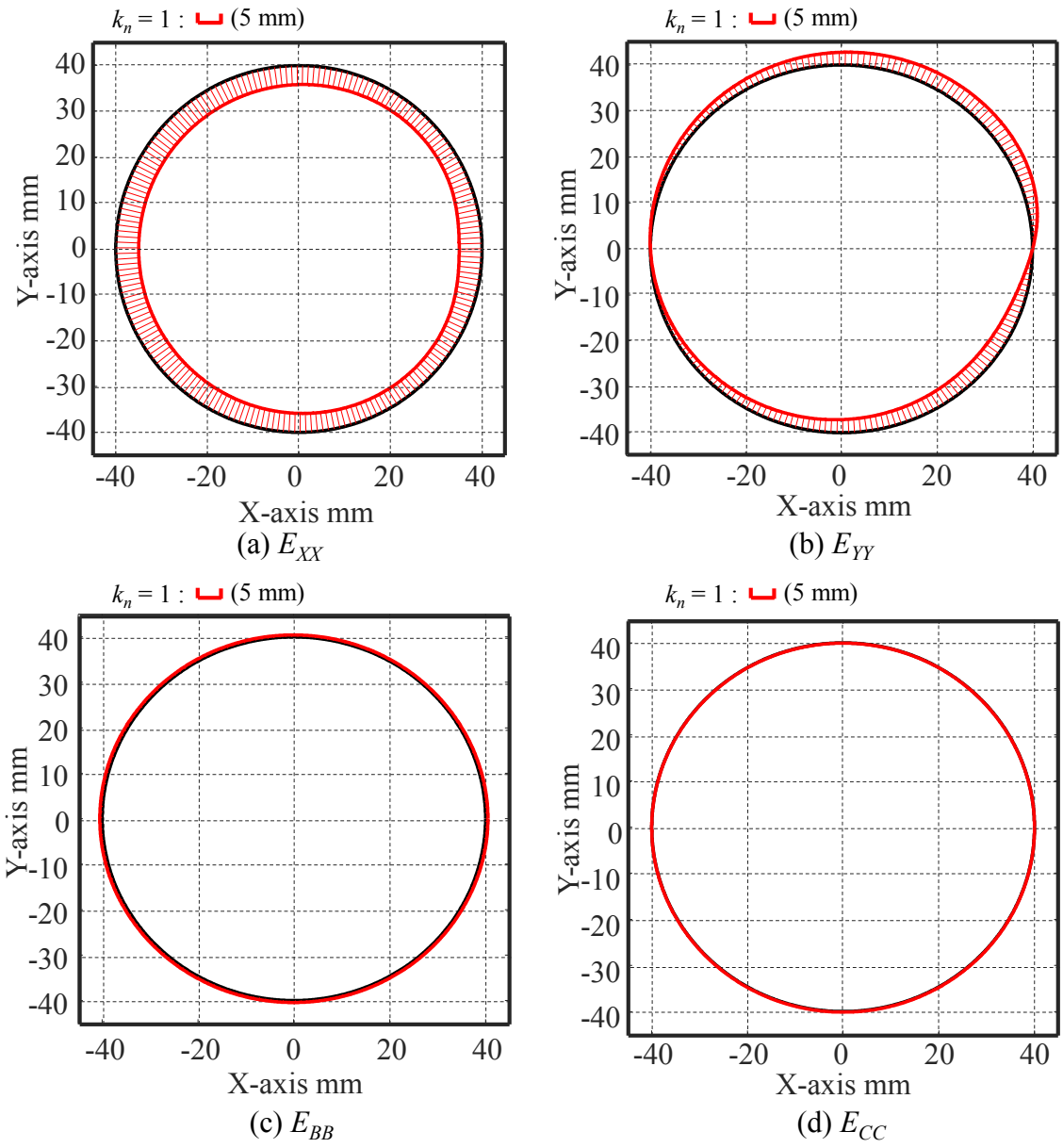

Figure 14 Sensitivity coefficient for each error motion for M3_15 test piece without offset.

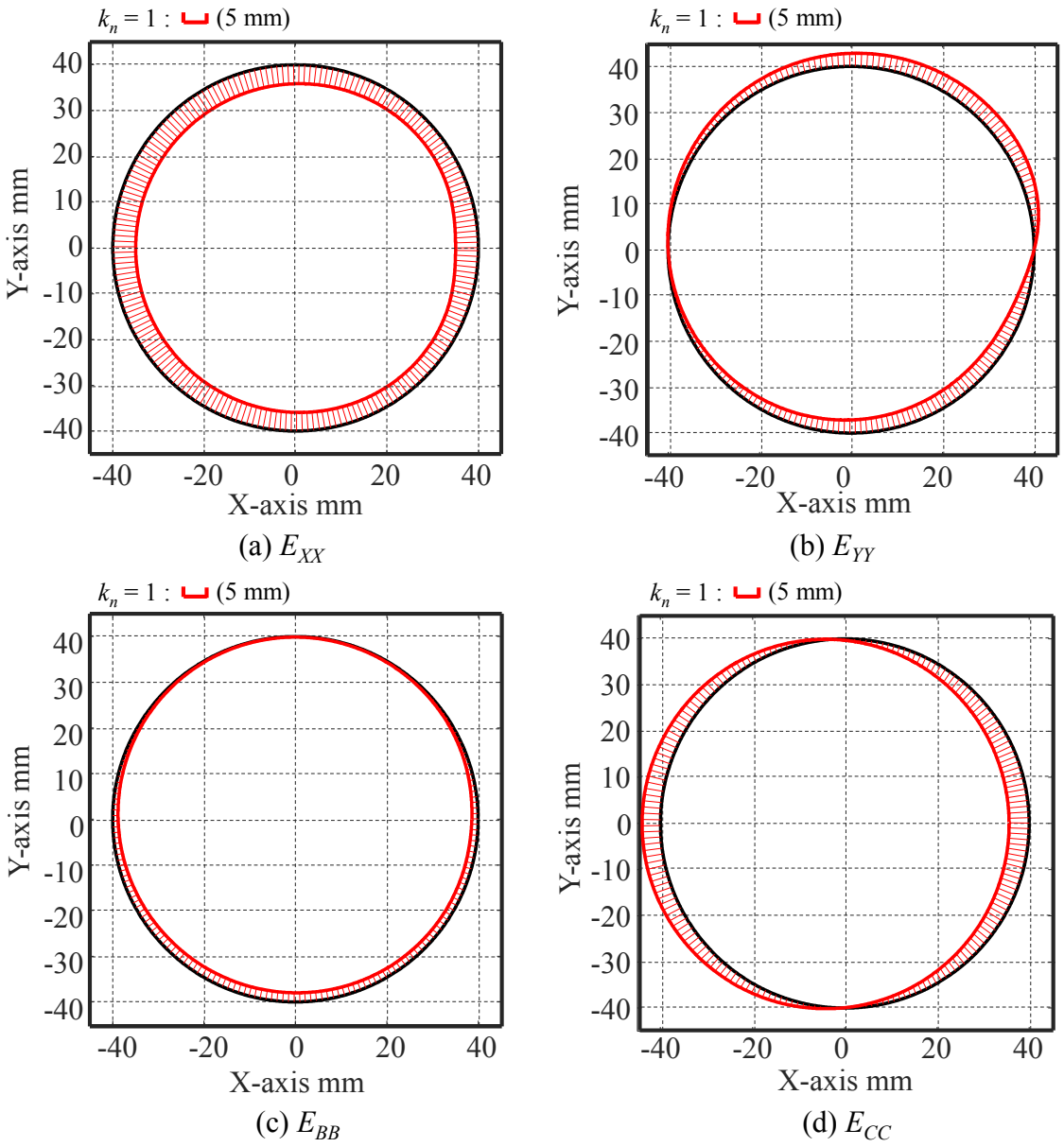

Figure 15 Sensitivity coefficient of each error motion for M3_15 test piece with offset.

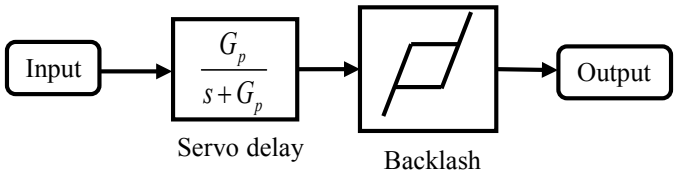

Figure 16 Model for simulating reversal errors.

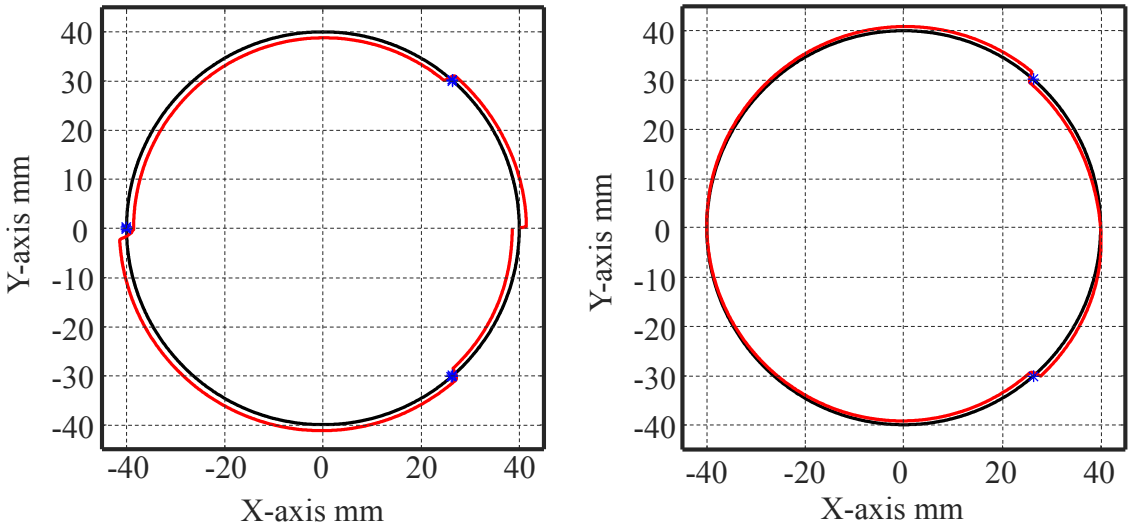

(a) X-axis reversal errors (b) Y-axis reversal errors

Figure 17 Results of simulation of reversal errors of each axis for M3_15 test piece without offset.

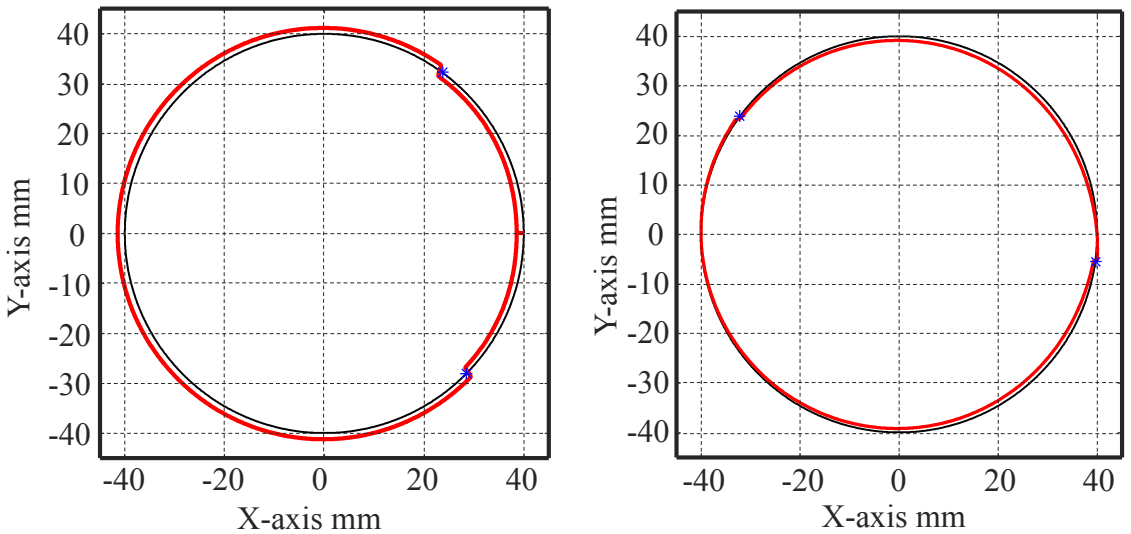

(a) X-axis reversal errors (b) Y-axis reversal errors

Figure 18 Results of simulation of reversal errors of each axis for M3_15 test piece with offset.

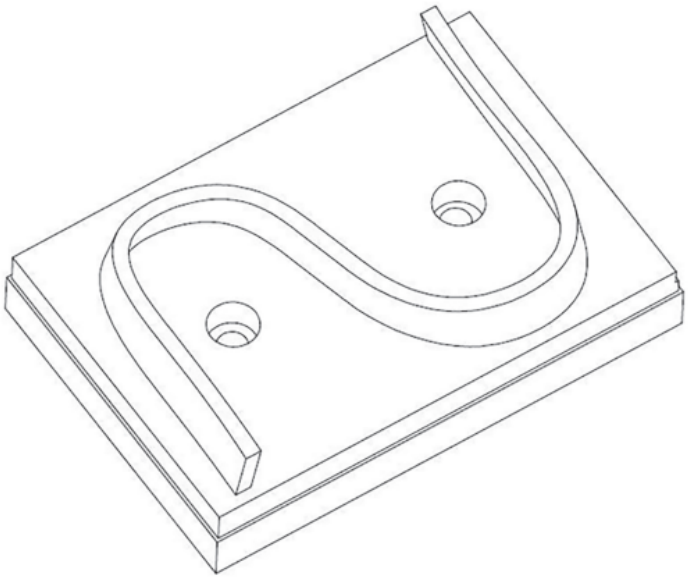

(a) Geometry used for S-shaped machining test [9].

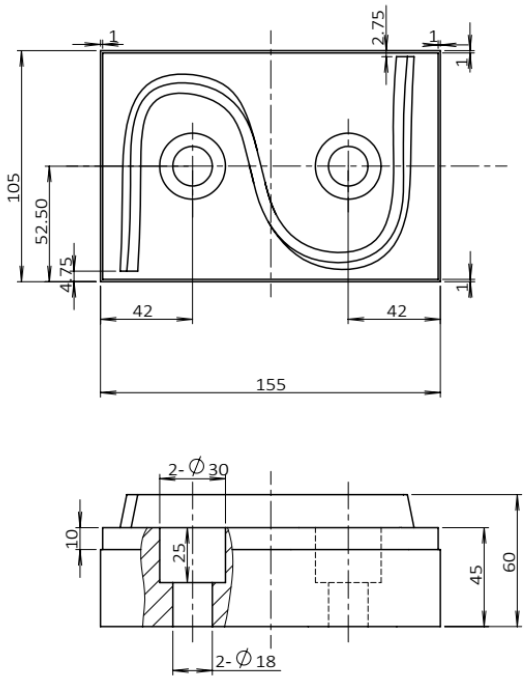

(b) Mechanical drawing of S-shaped machining test.

Figure 19 S-shaped machining test design.

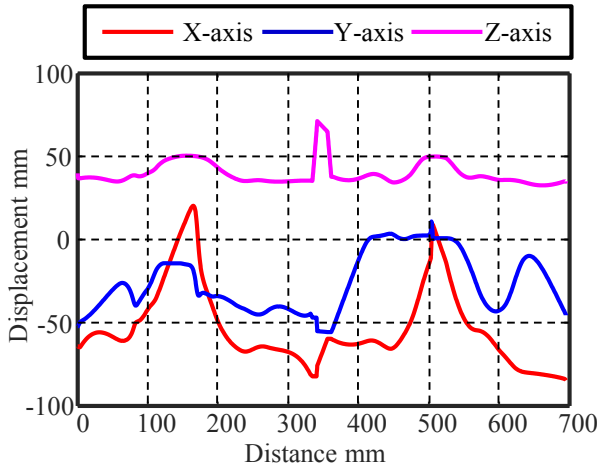

(a) Motions of translational axes

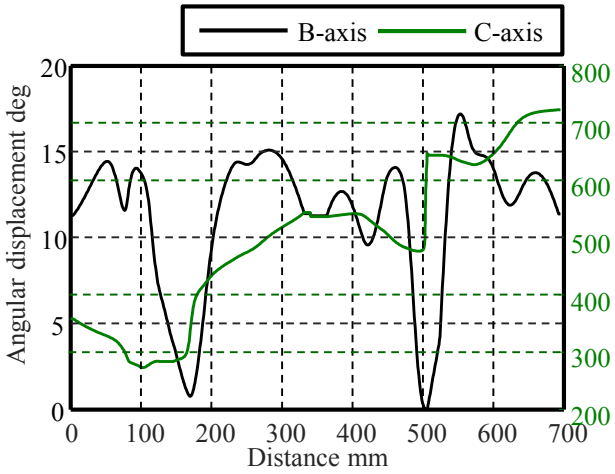

(b) Motions of rotary axes

Figure 20 Feed-axes motions during S-shaped machining test.

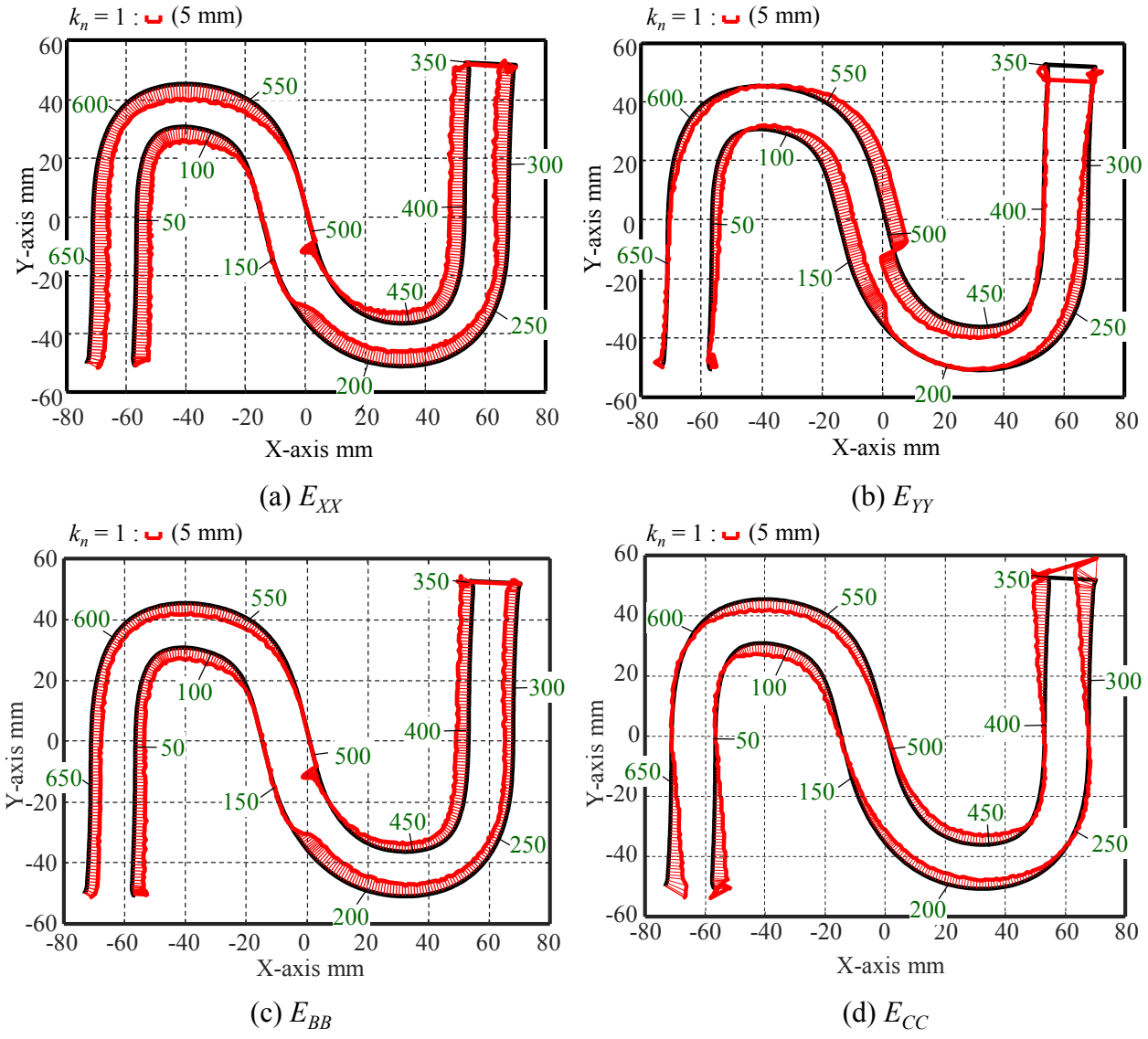

Figure 21 Sensitivity coefficient for each error motion for S-shaped machining test.

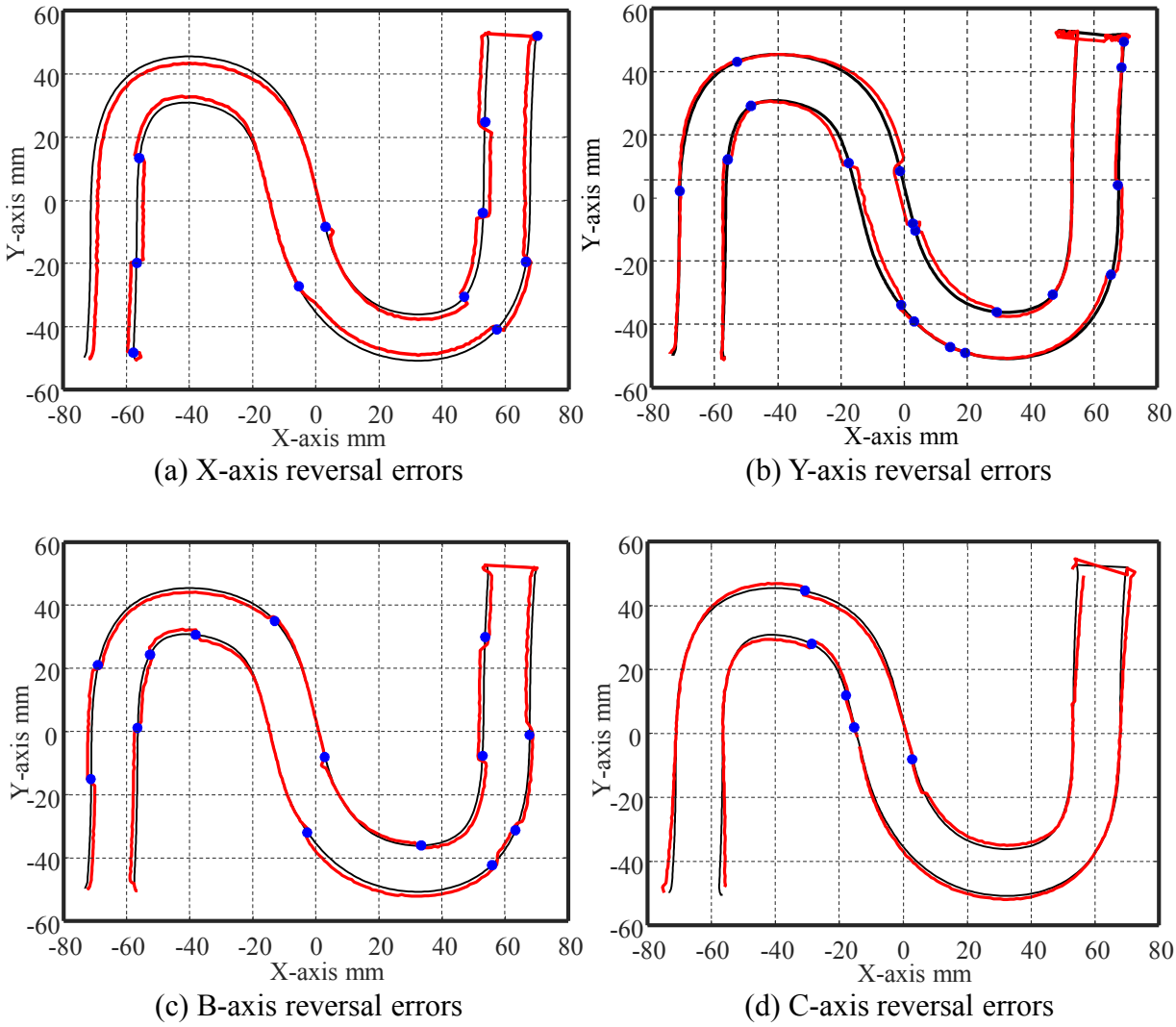

(a) X-axis reversal errors

(b) Y-axis reversal errors

(c) B-axis reversal errors

(d) C-axis reversal errors

Figure 22 Influence of reversal errors of each feed axis.